

NASA Technical Memorandum 106483

1N-35

205034

16P

Miniature Convection Cooled Plug-Type Heat Flux Gauges

Curt H. Liebert
Lewis Research Center
Cleveland, Ohio

Prepared for the
40th International Instrumentation Symposium
sponsored by the Instrument Society of America
Baltimore, Maryland, May 1-5, 1994

(NASA-TM-106483) MINIATURE
CONVECTION COOLED PLUG-TYPE HEAT
FLUX GAUGES (NASA) 16 p

N94-24069

Unclas

NASA

G3/35 0205034



MINIATURE CONVECTION COOLED PLUG-TYPE HEAT FLUX GAUGES

Curt H. Liebert

**National Aeronautics and Space Administration
Lewis Research Center
Cleveland, Ohio 44135**

KEYWORDS

Heat flux gauge

ABSTRACT

This work describes tests and analysis of a new miniature plug-type heat flux gauge configuration. This gauge can simultaneously measure heat flux on two opposed active surfaces when heat flux levels are equal to or greater than about 0.2 MW/m^2 . The performance of this dual active surface gauge was investigated over a wide transient and steady heat flux and temperature range. The tests were performed by radiatively heating the front surface with an argon arc lamp while the back surface was convection cooled with air. Accuracy is about ± 20 percent. The gauge is responsive to fast heat flux transients and is designed to withstand the high temperature (1300 K), high pressure (15 MPa), erosive and corrosive environments in modern engines. This gauge can be used to measure heat flux on the surfaces of internally cooled apparatus such as turbine blades and combustors used in jet propulsion systems and on the surfaces of hypersonic vehicles. Heat flux measurement accuracy is not compromised when design considerations call for various size gauges to be fabricated into alloys of various shapes and properties. Significant gauge temperature reductions (120 K), which can lead to potential gauge durability improvement, were obtained when the gauges were air-cooled by forced convection.

INTRODUCTION

The performance of a new plug-type dual active surface heat flux gauge configuration was studied using the radiant heat source of a powerful arc lamp. This dual gauge configuration is being developed for simultaneous measurement of local heat flux on two opposed active surfaces. One of the surfaces may be heated as the other surface is convection cooled. The gauge is machined into a metal specimen and is designed to withstand the high heat flux, temperature, pressure, erosive and corrosive environments generated in modern engines or on the surfaces of hypersonic vehicles.

Surface heat flux measurements and associated material temperature measurements have broad usefulness because they can aid in characterizing hot, hostile high pressure and temperature environments. This characterization is used to refine and verify material stress prediction codes and to aid in the modeling of the boundary layer state (ref. 1). The dual active surface heat transfer phenomena measured with the heat flux gauge relies upon steady or time dependent heat transfer to or from the two active surfaces of the gauge and upon heat conduction within the gauge.

The surface heat fluxes and temperatures are calculated from steady or transient temperature measurements obtained with thermocouples mounted at a minimum of three interior gauge locations.

The determination of heat flux on the surface of a conducting gauge body using internal temperature measurements is an application of the inverse heat conduction problem (ref. 2). The use of inverse heat conduction models is practical because it is relatively easy to accurately measure temperatures at interior gauge locations. Also, thermocouples enclosed within the gauge configuration are not in contact with corrosive and erosive environments. The design of the miniature dual active surface plug-type gauges investigated herein is based on the design of the durable uncooled single active surface gauges investigated in reference 1. The gauges described in reference 1 were used at NASA-Marshall Space Flight Center in a turbine blade tester which simulated nonrotating space shuttle main engine (SSME) turbopump turbine blade environmental conditions. In this tester, surface heat fluxes from about 0.3 to 21 MW/m² were measured at gas pressures from atmospheric to 15 MPa and gas temperatures from 90 to 1300 K. The gauges and blades within which the gauges were mounted were subjected in this tester to a severe and sudden increase in temperature and heat flux followed by an almost equally severe and sudden decrease in temperature. Time variations of heat flux on the order of 100 MW/m²-sec were measured in the SSME tester. (1 MW = 1 megawatt = 1×10⁶ watt.)

The work discussed herein is part of a broad research program for developing transient and steady heat flux measurement methods. This program is not only a fabrication program for developing durable heat flux gauges, but also a program for clarifying principles and for developing and verifying analytical tools for heat flux measurement. Reported herein are time and space variant, one-dimensional inverse heat conduction models and nonlinear analysis incorporating temperature variant properties for determining surface heat flux and surface temperature. The use of nonlinear analysis is very important for modern industrial applications where temperature gradients can be large and temperature changes can be rapid. The method is sufficiently general for application to many other inverse one-dimensional heat transfer problems.

Procedures for fabrication of dual active surface plug-type heat flux gauges, assessment of gauge durability and measurement quality and elements contributing to measurement uncertainties are also discussed. Depending upon the intended application, miniature dual active surface gauge lengths vary from 0.147 to 1.025 cm and overall gauge diameters vary from 0.290 to 0.574 cm. The experiments were made in a heat flux gauge calibration facility located at NASA Lewis Research Center. The gauges were operated over a transient and steady heat flux range of about 0.3 to 5.5 MW/m². Durability tests performed in the arc lamp were made as temperatures rose from 300 to 1500 K in 3 sec.

ANALYTICAL METHOD

A one-dimensional, inverse heat conduction method is formulated for obtaining heat fluxes and temperatures on two opposed surfaces of metal plug-type gauges using internal transient or steady temperature measurements. The method incorporates distributed heat transfer laws, i.e., laws whose terms depend on space. The variation of thermal properties with temperature is incorporated in this method. Temperature variant property values are taken from reference 3.

RATE EQUATIONS

Heat is defined as energy in transit. It is possible to quantify this concept of heat in terms of appropriate heat flux and heat balance rate equations associated with temperature gradients and temperature changes instantaneously measured within the gauge shown in figures 1 and 2. The required temperature measurements are made on the

thermoplug. The total length of the thermoplug includes a wall thickness, a cylindrical post length and a cover thickness. Because the post is thermally insulated on its cylindrical side, it is assumed that the gauge design allows for one-dimensional heat transfer in the thermoplug. Instantaneous one-dimensional heat conduction on the thermoplug is shown in figure 3. The direction from the front surface to the back surface of the thermoplug is considered positive.

Temperature Gradients (Fourier's Law) - As the thermoplug is heated on the front surface and cooled on the back surface, the thermoplug temperatures (T) and temperature gradients ($\partial T/\partial Z$) can vary with time in a nonlinear way along the length of the thermoplug. The heat flux (\dot{q}) associated with time variant or steady temperature gradients is (ref. 4)

$$\dot{q} = -k \left(\frac{\partial T}{\partial Z} \right), \text{ W/m}^2 \quad (1)$$

Equation (1) applies anywhere along the Z -axis of the thermoplug (fig. 1). Equation (1) also applies during transient or steady heat flow conditions. The thermal conductivity, k , of the thermoplug material can vary locally with temperature. The heat leaving the back surface of the thermoplug, where $Z = L$, is

$$\dot{q}_{\text{back}} = -k \left(\frac{\partial T}{\partial Z} \right)_{Z=L}, \text{ W/m}^2 \quad (2)$$

(Nomenclature is given at the end of this section.)

Temperature Changes (Heat storage) - As heat is transferred into and out of the front and back active surfaces of the thermoplug, the temperature of the thermoplug's mass can change with time. The rate of heat per unit volume required to change the temperature of a material from one temperature to another is (ref. 4)

$$\frac{\dot{Q}_{\text{store}}}{V} = \frac{m}{V} c_p \frac{\partial T}{\partial \theta}, \text{ W/m}^3 \quad (3)$$

where the mass, m , and specific heat, C_p , at constant pressure are allowed to vary with temperature and the partial derivative in equation (3) is called the temperature history. Because the mass per unit volume of the thermoplug material equals its density, equation 3 may be rearranged in terms of heat flux as

$$\dot{q}_{\text{store}} = \int_0^L \left[\rho c_p \frac{\partial T}{\partial \theta} \right] dZ, \text{ W/m}^2 \quad (4)$$

Heat Balance - A conservation of energy equation describing a heat balance on the thermoplug (fig. 3) in terms of transient or steady heat flux is

$$\dot{q}_{\text{front}} = \dot{q}_{\text{store}} + \dot{q}_{\text{back}}, \text{ W/m}^2 \quad (5)$$

Substituting equations (2) and (4) into (5) produces a heat flux equation for a thermoplug which is simultaneously heated at the front surface and cooled at the back surface

$$\dot{q}_{\text{front}} = \int_0^L \left[\rho c_p \frac{\partial T}{\partial \theta} \right] dZ + k \left(\frac{\partial T}{\partial Z} \right)_{Z=L}, \text{ W/m}^2. \quad (6)$$

where, for the tests performed herein, $\partial T/\partial \theta$ has a positive value and $\partial T/\partial Z$ has a negative value.

In equations (1) to (6), \dot{q}_{front} and \dot{q}_{back} are heat fluxes on the front and back surfaces, \dot{q}_{store} is heat flux associated with heat storage, \dot{Q}_{store}/V is time rate of change of stored heat per unit volume, ρ, C_p and k are temperature variant density, specific heat and thermal conductivity of the thermoplug material, T is internal gauge thermoplug temperature, θ is time, L is the thermoplug length measured from the front active surface to the back active surface and Z is a distance measured along the axis of the thermoplug.

A numerical illustration for determining the heat fluxes and temperatures on both surfaces is presented in Appendix A.

FABRICATION OF DUAL ACTIVE SURFACE PLUG-TYPE HEAT FLUX GAUGE

Figures 1 and 2 show a sideview and backview of a miniature dual active surface plug-type heat flux gauge. The fabrication techniques closely followed those presented in reference 1 for single active surface heat flux gauges (fig. 4(c)). The main geometrical difference between a single and dual active surface gauge is that for the latter, the cylindrical post shown in figure 1 is not only integral with the specimen material at the front surface, but is also attached to a cover plate on the back surface. For a single active surface gauge, the back cover plate is not attached to the thermoplug (fig. 4c). This cover plate was fabricated from the same or similar material within which the dual active surface gauge is mounted. A concentric annulus surrounds the side of the cylindrical post. The annulus was electrical discharge machined (EDM) only partially through the specimen. The EDM technique for simultaneously machining the post (plug) and the annulus into a material is described in reference 1. The back cover was secured by welding or brazing it to an end face of the post. High temperature ceramic is used to fill in the thermocouple passage (fig. 1), thereby trapping air, which is a good thermal insulator, within the concentric annulus. This structure is advantageous because it is not necessary to provide additional fabrication effort for welding or threading the cylindrical post into position.

There is shown in figures 1 and 2 a plurality of bare thermocouple thermoelement wires of nominal 0.0038 cm diameter that are obtained from commercial single-thermoelement sheathed thermocouple assemblies. These assemblies have a diameter of 0.025 cm. The thermoelement wires are fabricated by the manufacturer from either Chromel or Alumel material. Sheathing and underlying ceramic surrounding each thermoelement was stripped to expose 2 to 10 cm of bare wire. The ends of each Chromel and Alumel bare wire were spot welded together along the length and onto the surface of the post to form a hot junction. Welding the wires to the post surface, rather than embedding them in the material, offers minimal resistance to one dimensional heat flow through the thermoplug. The small diameter of each 0.0038 cm diameter bare thermocouple wire minimized unwanted heat leakage along the wires. The bare wires were routed through the annulus to the rear of the gauge. The wires are never in direct contact with a hostile outside environment. The associated sheathed thermocouple assemblies were spot-welded to the bottom of a groove EDM'ed into the specimen material at the rear of the gauge. The thermocouple assemblies were spot checked against standard temperature-millivolt curves to assure calibration accuracy.

Three to five thermocouple hot junctions were equally spaced visually around the cylindrical circumference at various distances from the front active surface of the gauges. Thermocouples were always placed at the front and

back of the post. The locations of the thermocouple hot junctions were determined with a toolmakers microscope. Table I shows the number of thermocouples attached to the thermoplugs.

MATERIALS AND GAUGE DIMENSIONS

The design of the dual active surface heat flux gauges for a particular application depends on the size, shape and type of material within which the gauge is mounted. Four applications are described in Table I. Table I in combination with figure 4 shows gauge dimensions, gauge materials and the number of thermocouples used on the various-sized thermoplugs. For gauge numbers 1 to 3, the thermocouples were always mounted onto the cylindrical surface of the post. The small annulus dimensions and post lengths given in Table I and figure 4 are constraints on the number of thermocouples which can be mounted on the post. The front surfaces of the plug-type gauges were covered with a black paint which has an absorptivity of 0.89.

ARC LAMP HEATING CHARACTERISTICS

Heat flux was provided with a Vortek arc lamp. The arc lamp was developed by Vortek Industries located in Vancouver, British Columbia, Canada. A plasma arc is contained within a quartz tube. Demineralized and pressurized water flows through the tube. The water cleans and cools the inner tube surface. A water cooled elliptical reflector focused thermal radiation from the arc onto a 1×4 cm rectangular test region. The test region was located in the test cell environment outside the reflector. The front active surface of a gauge specimen was automatically and accurately positioned at the test region with a high speed three-axis positioning system. A data acquisition system scanned the incoming data every 5 msec. This heat flux gauge facility is described in more detail in reference 5.

Factory calibrated water cooled asymptotic calorimeters were used as reference heat flux gauges during the development of the new miniature dual active surface plug-type gauges. These reference gauges were calibrated by the manufacturer (Hy-Cal Engineering, El Monte, California) only at steady heat flux conditions and therefore may not be reliable during transient heat flux measurements. Therefore a photodetector operating at 300 K was initially used to define the shape of the transient and steady heating curve generated by the arc lamp. The photodetector millivolt output is linearly proportional to the incident radiant energy intensity from the arc lamp. A typical heating curve shape is shown in figure 5. This shape was obtained by measuring arc lamp radiant energy reflected from a white test cell wall maintained at a temperature of 300 K. The reflectivity of the wall was uniform at the wavelengths of interest (0.3 to 1.5 μm). The photodetector temperature of 300 K was maintained by locating it at a large distance from the arc lamp.

The photodetector millivolt data presented in figure 5 established that the lamp idles for 0.3 sec. As shown in figure 5, the radiant energy output of the arc lamp is about 0.2 MW/m^2 at idle conditions. The lamp was designed by the manufacturer to idle at an idle current of 30 A. The resultant photodetector output shown in figure 5 is steady during this idle period. At 0.3 sec, a higher current was programmed into the lamp. In response to the higher current of 150 A, the millivolt output of the photodetector rises as shown in figure 5 through a transient start up time interval to a higher steady value and remains essentially steady until the lamp was shut down to the 30 A idle current condition. Other heating shapes (not shown) were obtained at 50 and 100 A. The level of steady radiant energy output attained after the transient startup period is higher at higher currents. The photodetector data also showed that the time for the startup transient is shorter at higher lamp currents.

After the shapes of the heating curves had been established with the photodetector, three water cooled Hy-Cal reference gauges were used to quantitatively measure the mean steady heat flux at three different steady arc lamp energy outputs. The steady heat fluxes were measured with the three gauges at 50, 100 and 150 A of lamp operating current and at gauge temperatures of 300 to 350 K. These steady heat fluxes were then analyzed using statistical analysis of mean values at a three-sigma level. The mean of all the steady heat fluxes measured with the three Hy-Cal reference gauges was 0.41, 1.03, 1.20 MW/m² and 5.5 MW/m² at arc lamp operating currents of 50, 100 and 150 A. These heat fluxes were chosen to match design estimates of the front surface heat flux associated with the various applications specified in Table I. Figure 5 shows the mean value of 1.20 MW/m² measured at the steady heat flux condition associated with a lamp current of 150 A. The uncertainty, i.e., confidence interval estimates of the steady heat flux of 1.20 MW/m² measured with the three reference gauges at 150 A is ± 8 percent. This value of ± 8 percent uncertainty at steady conditions was also measured at 50 and 100 A of lamp current.

The ± 8 percent level of steady heat flux measurement uncertainty is caused by electrical noise, arc flickering, nonuniform heat flux at the focus, lack of ability to repeatedly remove gauges from the calibrator and then reset them exactly at the focus, errors caused by the data processing equipment, errors caused by changes in the value of the absorptivity (0.89) of the black paint covering the Hy-Cal gauge active surfaces, and by the advertised accuracy of the reference gauges. From experience and manufacturer's data, the estimated maximum uncertainty of each of these elements is believed to be ± 3 percent which computes to a maximum rms (root-mean-square) uncertainty of about ± 8 percent. This rms uncertainty is consistent with the three-sigma calculation of 8 percent uncertainty discussed above giving support to the values used to estimate the uncertainty of each element associated with the rms calculation. The absorptivity changes of the black paint were measured with a reflectometer.

RESULTS AND DISCUSSION

Heat Flux Measured with Plug-Type Gauges

Gauges 1 and 2 - The mean steady heat flux measured at 150 A with plug-type gauges 1 and 2 (fig. 4 and Table I) is compared in figure 5 with the steady reference gauge measurements. The plug-type gauge data presented in figure 5 was obtained when forced convection air cooling was applied to the back surfaces of the two plug-type gauges. As shown in figure 5, the mean heat flux measurement on the front surfaces of the two plug-type gauges is 1.37 MW/m², ± 17 percent which compares well with the reference gauge measurements of 1.20 MW/m².

This 17 percent uncertainty is caused by those uncertainty elements previously discussed for the reference gauges (with reference gauge uncertainty element not included) plus additional uncertainties in material thermal properties, thermocouple measurement uncertainties, intrusiveness of the gauge in the material wall, inaccuracies of curve fitting procedures and variations during testing of the absorptance of the black paint covering the front active surfaces. The maximum estimated uncertainty of each the thermoplug temperature measurements is about ± 2 percent. The uncertainty of the other additional elements obtained from experience and the literature is about ± 5 percent. The maximum root-mean-square uncertainty incorporating all the elements is ± 14 percent, which compares well with the three-sigma uncertainty of 17 percent.

Comparison of columns A and B in Table I show that the length-to-diameter ratios of gauges 1 and 2 are 1.71 and 5.41, respectively. This leads to the observation that steady heat flux is, within experimental error, not a strong function of these miniature gauge sizes. Thus steady heat flux can be effectively measured even when design considerations call for miniature gauges of various sizes to be fabricated into alloys of various shapes.

At steady heat flux conditions, gauges 1 and 2 were also tested at passive cooling conditions where there is no forced convection cooling on the back surface. To prevent overheating of the front active surface which can cause spallation and oxidation of the black paint at temperatures above 520 K, these passive cooling tests were done at a steady lower lamp heat flux output of 1.03 MW/m^2 and at temperatures not exceeding 520 K. Reference and plug type gauge mean steady heat flux measurements compared within an acceptable ± 19 percent.

Comparisons of reference and plug-type gauge 1 to 4 outputs were made only when the paint absorptance of both gauges was $0.89, \pm 5$ percent. Because of spallation and oxidation, the paint absorptance rapidly decreases from 0.89 when the plug-type gauge front active surface temperature exceeds about 520 K. Therefore these experiments were conducted at plug-type gauge surface temperatures not exceeding 520 K. The changes in black paint absorptivity were measured with a reflectometer.

Transient heat flux data measured with gauges 1 and 2 are also presented in figure 5. Within an uncertainty of ± 20 percent, the transient heat flux history curve measured with both of these plug-type gauges follows the nonlinear shape of the lamp energy transient curve obtained with the photodetector. It is also shown in figure 5 that the start and end of the energy transient (rise time) agrees well with the start and end of the measured heat flux transient. This shows that the plug-type gauges are responding to these fast changes of heat flux. During lamp transient start up, good repeatability of heat flux measurements with and without active cooling was achieved with gauges 1 and 2.

Even though the reference Hy-Cal gauges are not calibrated for transient heat flux measurements, they never-the-less were also used to measure transient heat flux. The resulting data was compared to the plug-type heat flux measurements and the millivolt output of the photodetector. As seen in figure 5, values of transient heat fluxes measured with the reference gauges are consistent with the results obtained with the plug type and photodetector gauges. The results show that transient heat flux can be effectively measured when design considerations call for various size miniature plug type gauges to be fabricated in materials of various shapes.

Gauge 3 - Gauge 3, Table I, was tested at transient and steady heat flux conditions with active and passive cooling at 50 A of lamp operating current. The gauge displayed good transient and steady heat flux measurement correspondence (± 18 percent) with the reference gauges.

Gauge 4 - Because of space limitations within the annulus and on the post of these miniature gauges, only a limited number of thermocouples can be mounted on the post. Therefore a method for placing an additional thermocouple in the wall (denoted by F') in figure 4 of the gauge was devised and tested. A thermocouple was placed close to the front active surface by spot welding it to the bottom of a hole EDM'ed into the wall of gauge 4. The hole extended from the bottom of the annulus to within 0.015 cm of the front active surface of the gauge. The hole diameter was 0.024 cm. The bottom of the hole was located on the center line of the thermoplug. The empty region above the thermocouple hot junction was unavoidably filled with thermally insulating air which can possibly cause a hot spot at the thermocouple location. However this potential hot spot was not evident in these tests. Three thermocouples were also arc-welded to the post surface along its length. Heat fluxes over a range of about 0.41 to 5.5 MW/m^2 were measured and satisfactory agreement of steady and transient heat flux values measured with the reference and plug gauges was observed. (Data not shown.) Tests with three other single active surface gauges with varying wall thickness showed that satisfactory results are obtained when the wall thickness is greater than 0.031 cm.

Thermoplug Temperatures, Temperature Gradients and Active Surface Temperatures Using Active and Passive Cooling

Figure 6 presents temperature gradients measured along the length of the thermoplug of gauge 1 during active and passive gauge cooling. In general, the temperature gradients were nonlinear. It was found that the back surface heat

flux could not be accurately evaluated with equation (2) when data scatter about a least squares correlation temperature gradient curve was greater than 1 percent, when correlation coefficients were less than 0.97 and when the temperature drop was less than 2 percent. This occurred at dual active surface heat fluxes of 0.2 MW/m^2 or less.

Figure 6 shows, as expected, that higher thermoplug temperature levels are obtained when the back surface is passively cooled. The passive cooling was established by a small amount of convection in the relatively large forced convection cooling passage behind the back cover. The data shown in figure 6 were obtained at 0.8 sec when the lamp was operating at 150 A and at a 1.20 MW/m^2 level of heat flux. The lower thermoplug temperature level data shown in figure 6 were obtained at the same lamp current and at the same lamp operating time of 0.8 sec, but in addition with forced convection cooling air flowing along the back surface of gauge 1. The cooling air flow was about 0.34 kg/sec at an inlet air coolant temperature of 300 K and an inlet pressure of 0.7 MN/m^2 . Comparison of the upper and lower temperature gradients in figure 6 shows a significant reduction in gauge temperature of about 120 K when the pressurized cooling air is applied. This significant temperature reduction suggests that this design approach can provide substantial gauge cooling with the potential of improving gauge durability. Significant (100 K) temperature reductions were also noted when forced convection cooling was applied to gauges 2 and 3.

A least-squares power curve fit highly correlates (correlation coefficient, $r = 0.999$) the upper passive cooling thermoplug temperature gradient data shown in figure 6. However, the equation of a power curve fit can not be evaluated for front surface temperature at $Z = 0$. Therefore a slightly less accurate ($r = 0.978$, fig. 6) linear least-squares equation which can be evaluated at $Z = 0$ is fit through the data and a front active surface temperature of about 550 K was calculated. It is also shown in figure 6 that the use of the less accurate linear curve fit leads to an error of back surface temperature calculation of only 1.4 percent. More data obtained with gauges 1 to 3 at other heat flux levels and cooling conditions showed that estimation of front and back surface temperatures (using curve fits which can be evaluated at $Z = 0$) is relatively insensitive to the type of curve fit used when r ranges from 0.978 to 0.999 and when the equations fit the measured temperature data with a deviation of 1 percent.

After the tests discussed above were completed, the black paint on the front active surfaces of the gauges was removed and durability tests were performed on the gauges. No deleterious effects were noted when the gauges were heated from 300 to 1400 K in 3 sec.

CONCLUDING REMARKS

The results of measuring heat flux with new miniature dual active surface plug-type heat flux gauges and older single active surface heat flux gauges are presented and compared with transient and steady commercial heat flux gauge and photodetector measurements. At heat fluxes equal or greater than 0.2 MW/m^2 , the results show good measurement comparison (± 20 percent or less) over a wide range of gauge size, specimen material shapes and temperature. Gauge diameters range from 0.29 to 0.54 cm and gauge lengths range from 0.147 to 1.025 cm. No metal alloy or thermocouple durability problems were observed when the gauges were heated from 300 to 1400 K in 3 sec. The inverse, distributed and time variant conduction model formulated to estimate heat flux and temperature on the two active surfaces was found to be reasonably accurate and tractable while not posing a difficult analytical problem. Significant gauge temperature reductions were obtained when the gauges were air-cooled by forced convection.

APPENDIX—ILLUSTRATION OF CALCULATION METHOD USING DUAL ACTIVE SURFACE GAUGE 1, TABLE I

An example of using a numerical method for solving equation (6) is presented. Use of least-squares curve-fit equations to describe variations of pertinent variables is discussed in this section. This section numerically illustrates how the gauge works. The numerical method has been programmed into hand-held calculators and computers.

Internal gauge temperature data taken with gauge 1 at 150 A and 0.8 sec are used in this example. These data were obtained when forced convection cooling was applied along the back surface. The curve fits used herein describe straight line, parabolic, exponential and power equations. When the heat fluxes have been determined, the heat conduction equation (eq. (6)) is solved.

Temperature Gradients - The following steps are used to illustrate the evaluation of the second and third terms on the right hand side of equation (6) when using the temperatures measured with three thermocouples located along the surface of the cylindrical post at 0.033, 0.071 and 0.112 cm distance from the front active surface.

Step 1. Consider evaluation of \dot{q}_{back} in equation (6) which expresses back surface heat flux as thermal conductivity times temperature gradient evaluated at the back surface (eq. (2)). The lower curve in figure 6 shows a plot of the temperatures measured at three thermocouple locations along the thermoplug length. These three temperatures are correlated with an exponential least squares curve fit. The curve fit criteria is such that the equations should fit the measured temperature data within a deviation of one percent and with corresponding correlation coefficients of 0.990 or larger. Using the resulting curve fit equation, the temperature at the actively cooled back face of the thermoplug where $Z = L @ 0.147$ cm is extrapolated and calculated with this curve fit equation as 385 K. The value of k for Inconel 718 at this temperature is 12.2 W/mK.

Step 2. The numerical value of the derivative at $Z = L$ of the least-squares exponential curve fit equation is -26000 K/m. Thus, at $Z = L$, $\dot{q}_{\text{back}} = -(12.2 \text{ W/mK})(-26000 \text{ K/m}) = 0.32 \text{ MW/m}^2$, (eq. 2).

Temperature Changes

Step 3. Consider evaluation of \dot{q}_{store} in equation (6) at the same three temperature measurement locations and again at time equals 0.8 sec. This involves solving equation (4) in terms of local temperature history with thermal properties a function of temperature. A plot of the three transient temperature histories obtained with the three thermocouples mounted on the post is shown in figure 7. The temperature recorded at 0.8 s by the thermocouple located at $Z = 0.033$ cm is 406 K. At this temperature, the values of density and specific heat of Inconel 718 are 8193 kg/m^3 and 448 J/kg-K .

Step 4. Evaluate the derivative of temperature with respect to time at this 0.033 cm location and at time equals 0.8 sec. To do this, first fit the thermoplug temperature rise data measured over the range of 0.60 to 1.04 sec with the parabolic least-squares equation shown in figure 7. The value of the partial derivative of temperature with respect to time at 0.8 sec is 224.1 K/s.

Step 5. Multiplying the values for the density and specific heat of the thermoplug by the value of the derivative found in step 4 gives a value of 822.6 MW/m^3 for the rate of change of energy per unit volume (fig. 8). This value is plotted in figure 8 at $Z = 0.033$ cm. Proceeding in the same way, values of the rate of change of energy per unit

volume equal to 756 and 722 MW/m³ are calculated with equation (3) and plotted in figure 8 at the other thermocouple locations of Z = 0.071 and 0.112 cm, respectively.

Step 6. Now evaluate equation (4). The three values of rate of change of energy per unit volume as a function of thermocouple location on gauge 1 are connected with straight lines to form an irregular polygon bounded by the straight line through the data points and by the x and y axes as shown in figure 8. The enclosed area of the polygon is equal to the heat flux associated with the energy stored when arc lamp current equals 150 A at 0.8 sec of lamp running time. This stored energy is 1.14 MW/m³.

Instantaneous Heat Balance

Step 7. Evaluate the heat flux on the front surface using equation (6). The front surface heat flux is equal to the sum of 0.32 and 1.14 MW/m². This sum equals 1.46 MW/m².

Front Surface Heat Flux History

Step 8. Steps 1 through 7 are repeated to obtain front surface heat flux at other lamp operation times.

Front Surface Temperature

Step 9. As shown by the lower curve in figure 6, the extrapolated front active surface temperature at time equal 0.8 sec and 150 A is 425 K. This temperature is calculated using the least squares exponential curve fit equation for the temperature gradient at Z = 0. When compared with the method based on Fourier's law for obtaining surface temperature given in reference 1, the uncertainty of the extrapolated temperature is ±3 percent or less. Steps 1 through 8 can then be repeated to obtain dual active surface temperatures at other lamp operating times and other lamp currents.

REFERENCES

1. Liebert, C.H.: "Miniature High Temperature Plug-Type Heat Flux Gauges". NASA TN-105403, 1992.
2. Beck, J.V., et.al.: "Inverse Heat Conduction". John Wiley and Sons, Inc. 1985.
3. "Aerospace Structural Metals Handbook." Metals and Ceramics Information Center, Battelle Labs, Columbus, OH, 1989.
4. Eckert, E.R.G.; and Drake, R.M., Jr.: "Analysis of Heat and Mass Transfer". McGraw-Hill Book Company. 1972.
5. Liebert, C.H.; and Weikle, D.H.: "Heat Flux Measurements". NASA TM-101428. 1989.

Table I
Description of Gauges (see figure 4)

Gauge number	Gauge descriptions	Material	Thermo-plug length, cm, A or A'	Thermo-plug diameter, cm, B or B'	Annulus outside diameter, cm, C or C'	Annulus spacing, cm, D or D'	Post length, cm, E or E'	Wall thickness, cm	Number of thermocouples
1	Dual active surface gauge mounted in a convection cooled flat plate wall	INCONEL 718	0.147	0.086	0.290	0.102	0.086	0.028	3
2	Dual active surface gauge mounted in a convection cooled turbine rotor segment	MAR-M-247	0.373	0.069	0.315	0.123	0.305	0.023	5
3	Dual active surface gauge mounted in a convection cooled pipe bend	SS-E-316 H	1.025	0.180	0.574	0.197	0.864	0.091	5
4	Single active surface gauge mounted in square coupon	MAR-M-246	0.292	0.071	0.406	0.088	0.264	0.031	4

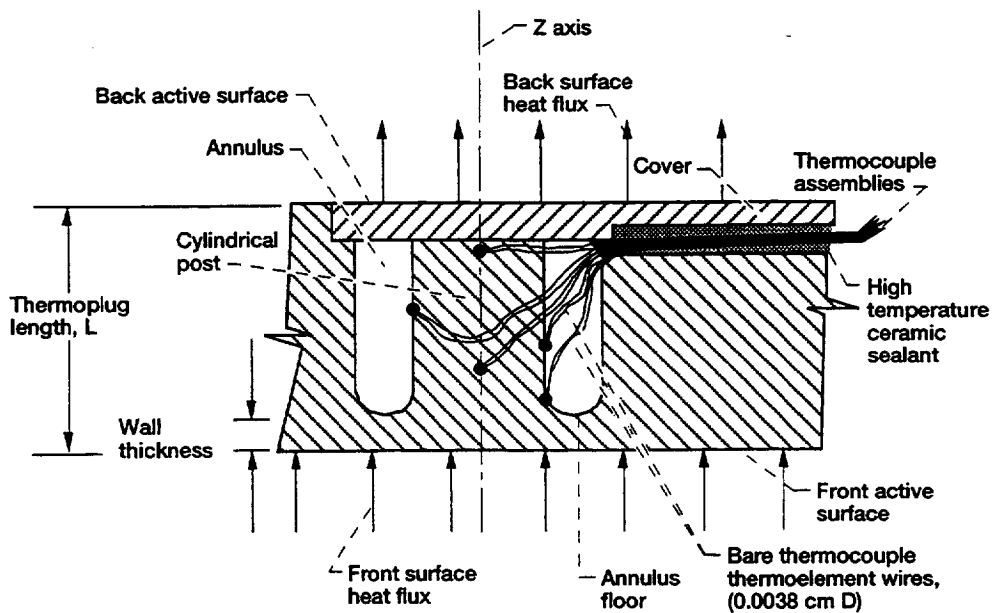


Figure 1.—Sideview of a typical miniature dual-active surface plug-type heat flux gauge.

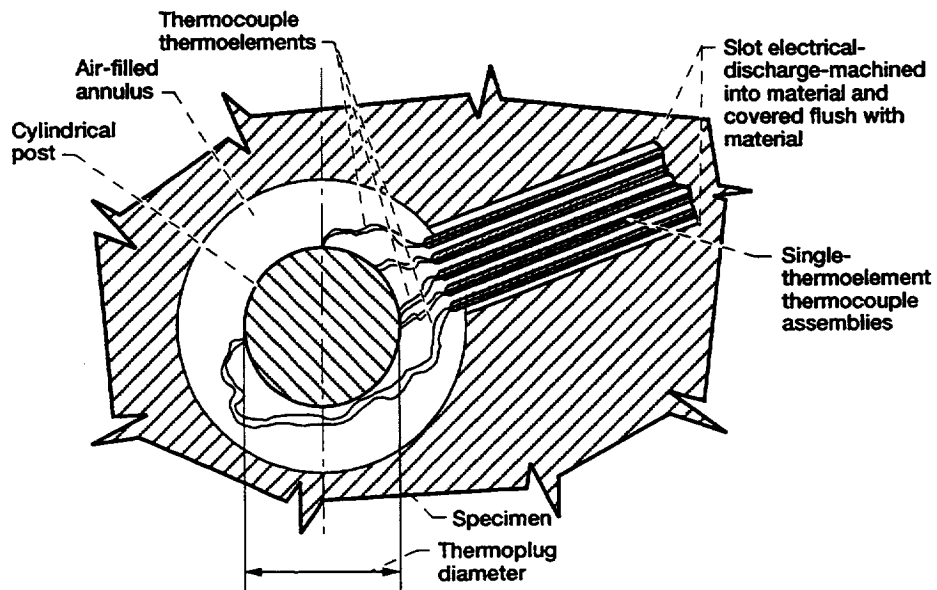


Figure 2.—Backview of a typical miniature dual active surface plug-type heat flux gauge (cover removed).

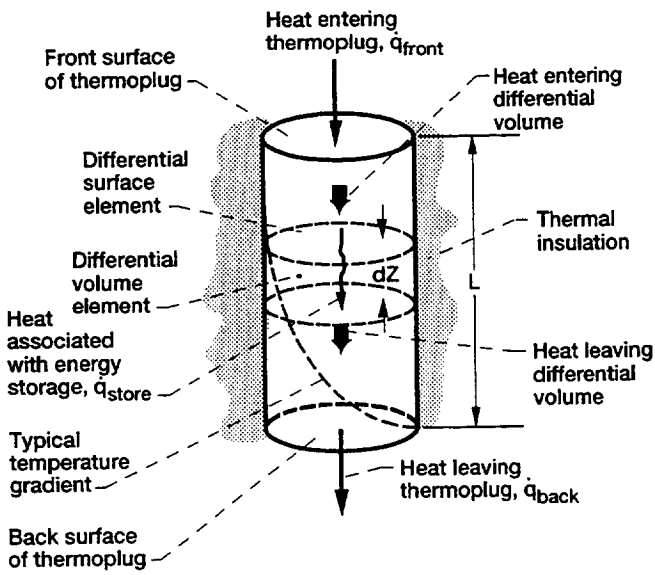


Figure 3.—Conduction in thermoplug.

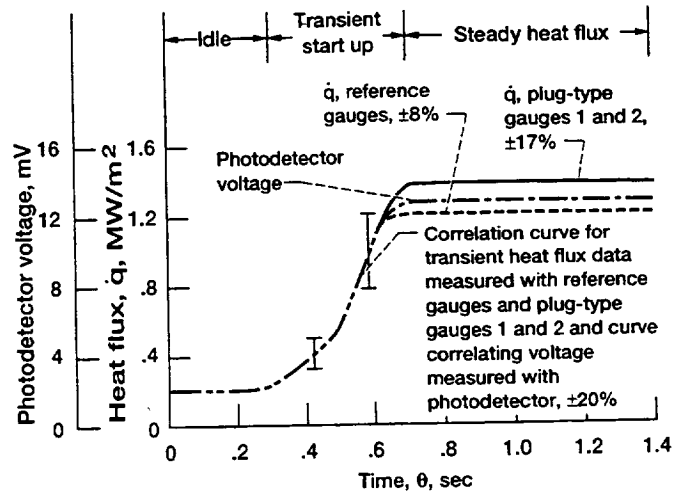


Figure 5.—Comparison of plug-type gauges 1 and 2 and reference gauge front surface heat flux measurements (150 A) (active cooling).

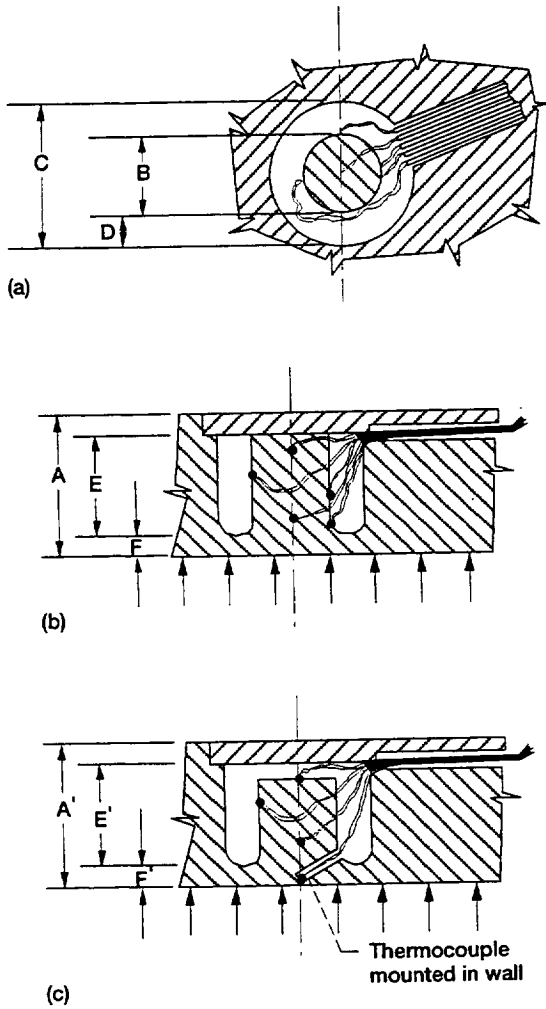


Figure 4.—Nomenclature for Table I. (a) Dual (gauges 1, 2 & 3) and single (gauge 4) active surface gauges. (Number of thermocouples varies from 3 to 5.) (b) Dual (gauges 1, 2 & 3) active surface gauge. (Number of thermocouples varies from 3 to 5.) (c) Single (gauge 4) active surface gauge.

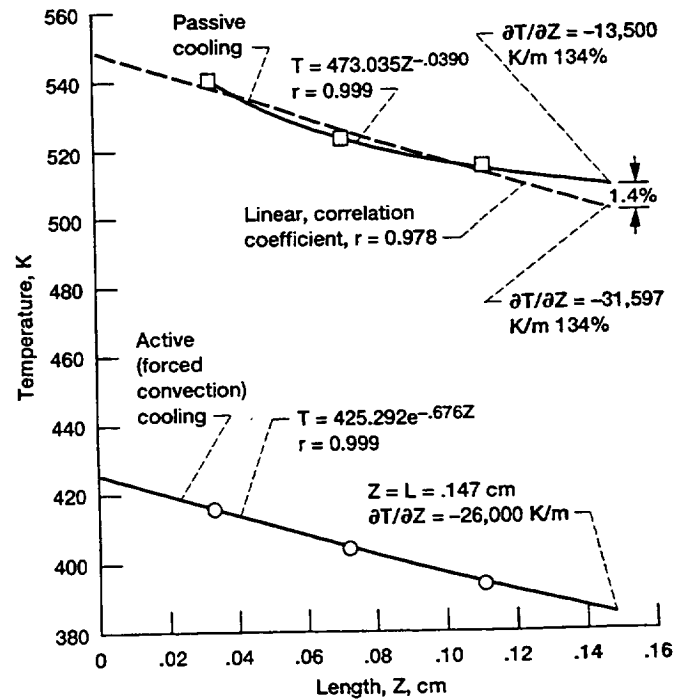


Figure 6.—Temperature gradients of plug-type gauge 1 at 0.8 sec (150 A).

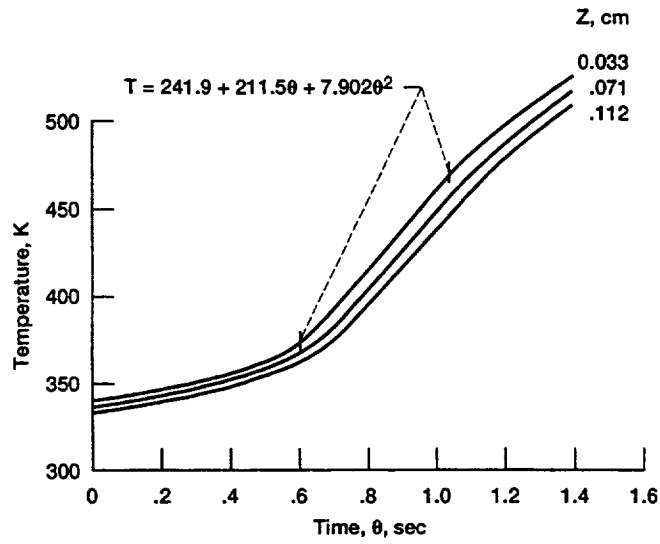


Figure 7.—Internal temperature histories of gauge 1 (150 A) (active cooling).

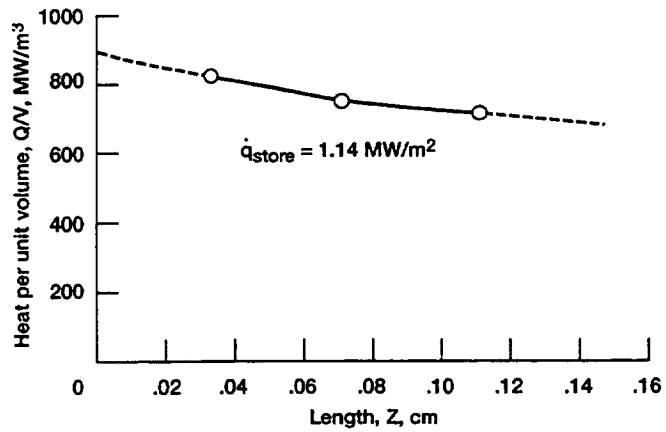


Figure 8.—Stored heat per unit volume and associated heat flux for gauge 1 at 0.8 sec (150 A) (active cooling).

REPORT DOCUMENTATION PAGE

Form Approved
OMB No. 0704-0188

Public reporting burden for this collection of information is estimated to average 1 hour per response, including the time for reviewing instructions, searching existing data sources, gathering and maintaining the data needed, and completing and reviewing the collection of information. Send comments regarding this burden estimate or any other aspect of this collection of information, including suggestions for reducing this burden, to Washington Headquarters Services, Directorate for Information Operations and Reports, 1215 Jefferson Davis Highway, Suite 1204, Arlington, VA 22202-4302, and to the Office of Management and Budget, Paperwork Reduction Project (0704-0188), Washington, DC 20503.

1. AGENCY USE ONLY (Leave blank)		2. REPORT DATE February 1994	3. REPORT TYPE AND DATES COVERED Technical Memorandum	
4. TITLE AND SUBTITLE Miniature Convection Cooled Plug-Type Heat Flux Gauges			5. FUNDING NUMBERS WU-505-62-50	
6. AUTHOR(S) Curt H. Liebert				
7. PERFORMING ORGANIZATION NAME(S) AND ADDRESS(ES) National Aeronautics and Space Administration Lewis Research Center Cleveland, Ohio 44135-3191			8. PERFORMING ORGANIZATION REPORT NUMBER E-8420	
9. SPONSORING/MONITORING AGENCY NAME(S) AND ADDRESS(ES) National Aeronautics and Space Administration Washington, D.C. 20546-0001			10. SPONSORING/MONITORING AGENCY REPORT NUMBER NASA TM-106483	
11. SUPPLEMENTARY NOTES Prepared for the 40th International Instrumentation Symposium sponsored by the Instrument Society of America, Baltimore, Maryland, May 1-5, 1994. Responsible person, Curt H. Liebert organization code 2510, (216) 433-6483.				
12a. DISTRIBUTION/AVAILABILITY STATEMENT Unclassified - Unlimited Subject Category 35			12b. DISTRIBUTION CODE	
13. ABSTRACT (Maximum 200 words) This work describes tests and analysis of a new miniature plug-type heat flux gauge configuration. This gauge can simultaneously measure heat flux on two opposed active surfaces when heat flux levels are equal to or greater than about 0.2 MW/m ² . The performance of this dual active surface gauge was investigated over a wide transient and steady heat flux and temperature range. The tests were performed by radiatively heating the front surface with an argon arc lamp while the back surface was convection cooled with air. Accuracy is about ±20 percent. The gauge is responsive to fast heat flux transients and is designed to withstand the high temperature (1300 K), high pressure (15 MPa), erosive and corrosive environments in modern engines. This gauge can be used to measure heat flux on the surfaces of internally cooled apparatus such as turbine blades and combustors used in jet propulsion systems and on the surfaces of hypersonic vehicles. Heat flux measurement accuracy is not compromised when design considerations call for various size gauges to be fabricated into alloys of various shapes and properties. Significant gauge temperature reductions (120 K), which can lead to potential gauge durability improvement, were obtained when the gauges were air-cooled by forced convection.				
14. SUBJECT TERMS Heat flux gauge			15. NUMBER OF PAGES 15	
			16. PRICE CODE A03	
17. SECURITY CLASSIFICATION OF REPORT Unclassified	18. SECURITY CLASSIFICATION OF THIS PAGE Unclassified	19. SECURITY CLASSIFICATION OF ABSTRACT Unclassified	20. LIMITATION OF ABSTRACT	